

A Method for Health Monitoring of Power MOSFETs Based on Threshold Voltage

Lei Ren

College of Automation Engineering
Nanjing University of Aeronautics & Astronautics
Nanjing, China
renleiNUAA@163.com
Chunying Gong
College of Automation Engineering
Nanjing University of Aeronautics & Astronautics
Nanjing, China

Qian Shen

College of Automation Engineering
Nanjing University of Aeronautics & Astronautics
Nanjing, China
Huizhen Wang
College of Automation Engineering
Nanjing University of Aeronautics & Astronautics
Nanjing, China

Abstract—The prognostics and health management (PHM) of airborne equipment plays an important role in ensuring the security of flight and improving the ratio of combat readiness. The widely use of electronics equipment in aircraft is now making the PHM technology for power electronics devices become more important. It is the main circuit devices that are proved to have high failure rate in power equipment. This paper does some research about the fault feature extraction of power metal oxide semiconductor field effect transistor (MOSFET). Firstly, the failure mechanism and failure feature of active power switches are analyzed in this paper, and the junction temperature is indicated to be an overall parameter for the health monitoring of MOSFET. Then, a health monitoring method based on the threshold voltage is proposed. For buck converter, a measuring method of the threshold voltage is proposed, which is simple to realize and of high precision. Finally, the simulation and experimental results verify the effectiveness of the proposed measuring method.

Keywords—The prognostics and health management (PHM); MOSFET; the failure mechanism; junction temperature; Buck converter; threshold voltage

I. INTRODUCTION

The development of power electronic converters (PECs) has led to their widespread use in many fields such as industry, military and aerospace due to their low noise, high efficiency, high power density and other advantages. With the growth of complexity and power levels of PECs, especially in the field of aerospace, the reliability of power electronic system has more and more received scholars' attention. The power electronic system often consists of main circuit and control circuit. As the main circuit operates at high switching frequency and high power, the decline of power devices is far faster than the control circuit which is composed of electronic circuits. Therefore, it's of great importance to perform PHM research of the main power supply devices. A failure survey of various components in a power converter shown in Fig.1 [1] clearly demonstrates that electronic capacitors and MOSFETs are the most age-affected components in power converter circuits.

With a deeper knowledge of the failure mechanism of electronic capacitors, extensive research has been conducted in recent years. However, since degradation in electronics is more

difficult to detect and inspect and fault in PEC may not necessarily lead to failure or loss of designated electrical performance or functionality, it is difficult to quantify degradation and the progression from faults to final failure. In addition, there is a significant shortage of knowledge about the unified failure precursors in power semiconductors.

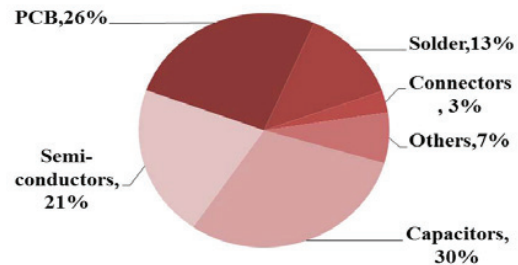


Fig. 1. Failure survey of different components responsible for converter failure[1].

Several projects have been carried out in recent years to understand and improve power device reliability. Most of the work in recent years has concentrated on insulated gate bipolar transistors (IGBTs) for power electronic converters. Some projects investigated the reliability of IGBT modules for traction applications, including IGBT bond wire liftoff, solder fatigue, and other reliability issues in traction applications [2-3], the results of which have been used in later work[4-5]. Some projects contributed to IGBT technology by improving the reliability tests and by achieving agreement on standardized accelerated tests[6]. There are also projects covering a range of reliability areas, such as lead-free soldering, accelerated testing, failure analysis, and thermal management. Power devices are included, for example, investigation into failure precursors for IGBTs[7].

The efforts outlined above are only for one single device and mainly for IGBTs. However, Power semiconductors are often equipped in a power electronic converter in an actual application. Furthermore, it is even more challenging when components need to be characterized while they are energized in a live converter, and conventional measurement techniques

This work was supported by the National Natural Science Foundation of China (51377079).

could not be used with ease. Therefore, two hurdles need to be crossed: 1. Since different degradation mechanisms may cause different degradation features, failure precursors are difficult to unify; 2. Present extraction circuits for failure precursors are quite complicated which will not only increase system's cost, but also reduce system's reliability.

This paper is organized in the following manner. Section II describes the origin of power MOSFETs failure and the measurable failure precursors which can quantify the level of aging. On this basis, one common degradation feature is pointed out: causing junction temperature to rise. Given this, the junction temperature is chosen as an overall indicator for health monitoring. According to the temperature sensitivity, the threshold voltage of MOSFETs is chosen as the thermo-sensitive electrical parameter for the junction temperature estimate. Section III demonstrates the proposed monitoring method which is based on the measurement of the threshold voltage. Besides, aiming at Buck converter, a simple threshold voltage measurement method is proposed. Section IV presents the simulation and experimental results for measuring threshold voltage of MOSFETs, which confirms the validity of the proposed measurement method. The summary has been presented in Section V.

II. ANALYSIS AND UNIFICATION OF FAILURE PRECURSORS FOR MOSFET

A. Failure Mechanisms and Failure Precursors

One of the most failure prone components in a power electronic converter is the power MOSFET. Fig.2 shows the equivalent circuit of a N-channel MOSFET whose three electrodes are drain electrode (D), gate electrode (G) and source electrode (S) respectively. In this diagram: R_g and R_{be} are parasitic resistances; C_{gd} , C_{gs} and C_{ds} are parasitic junction capacitors; D_1 is parasitic diode. In order to conduct a failure study and predict the remaining life of the single component as well as the entire converter, the mechanisms of these failures and previous work on the failure precursors induced by the degradation of power MOSFETs are described in the following section. In general, failure of semiconductor devices can be categorized into two groups: chip-related failure mechanisms and package-related failure mechanisms.

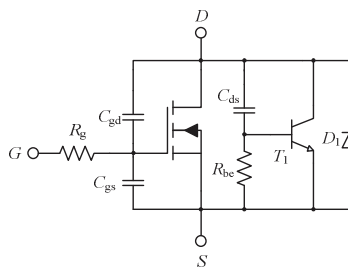


Fig. 2. Equivalent circuit of N-channel MOSFET.

Chip-related failure mechanisms are ultimately those that destroy a device. They are separated from packaging-related mechanisms, but may be interlinked for a failure event. The reasons for chip-related failures are electrical overstress,

electrostatic discharge, latch-up and triggering of parasitics, charge effects, and radiation effects[8]. Electrical overstress is associated with overvoltage and overcurrent conditions and heating effects may be too crucial to cause secondary breakdown. Such breakdown will lead to increased power dissipation and eventual thermal damage. Electrostatic discharge can partially puncture the gate oxide, which will cause gate shorting finally, and such failure can be detected by measuring the time constant of the decay of gate charge [9]. It was also found that the threshold voltage increases with aging [10]. Too large a value of dv/dt during turn off may cause triggering of the parasitic bipolar junction transistor in power MOSFETs, which may cause the shoot-through phenomenon in a bridge converter. Ionic contamination and hot carrier injection are the most common failure mechanisms for power MOSFETs. The first is the electric field distortion by the accumulation of ionic contaminants in the passivation of the high-field region, the second is the growth of defects in the gate oxide [9]. These two charge effects lead to shifting in the device performance characteristics — such as the threshold voltage (the most common), leakage current, transconductance, and saturation current. And in general, the threshold voltage shifts from the initial value because of any degradation in the gate oxide region and the amount of the shift depends on the amount of the interface trapped charge and the oxide trapped charge which are caused by the two charge effects. In an N-channel MOSFET, interface trapped charge makes the threshold voltage negative drift and oxide trapped charge is converse. However, most research suggests that oxide trapped charge will be dominant with aging, which means that the threshold voltage increases with aging. In addition, when threshold voltage is increased over cumulative stress, the gate to source capacitance C_{gs} decreased, and the gate to drain capacitance C_{gd} increased [12].

The packaging-related failures are most due to the dissimilarity between the coefficients of thermal expansion (CTE) of chip and the package. The two types of failures are bond failures and die solder layer failure. Bond failure is mainly caused by any crack at the bond wire/interface due to the difference of CTEs of Si and Al. On-state resistance $R_{DS(on)}$ of a MOSFET increased because of the degradation at metallization and at the contact area of bonding wire metallization [13]. Die solder layer failures are mainly caused by the difference of CTEs of Si and Cu (substrate). The induced voids increase the thermal resistance, resulting higher operating junction temperature. The thermal resistance can be detected from the junction temperature of the device indirectly.

Therefore, the main failure precursors associated with MOSFETs are 1) threshold voltage; 2) junction capacitors in the MOSFET equivalent circuit; 3) on-resistance; 4) thermal resistance.

B. Analysis of failure precursors

Power MOSFET is an electronic device used for the conversion of electrical energy, where unavoidable loss will cause its temperature to rise. Therefore, when we carry out the reliability investigations based on the failure precursors, the temperature characteristics of failure precursors should be taken into consideration, especially for real-time monitoring.

This section analyzes temperature property of the failure precursors mentioned above, and points out some issues that need attention.

1) On-state resistance-based research

From the existing literature study, it can be found that the $R_{DS(on)}$ is the most used failure precursor for MOS devices and the novelty in any technique lies in how accurately and conveniently it can be measured, especially when the device is energized. However, for on-line $R_{DS(on)}$ measurements, the dissipated power produced by both conduction and switching losses will cause the junction temperature to rise. And as known to us, $R_{DS(on)}$ has the property of positive temperature, which means the values measured online and offline are distinct for the same device. The relationship between the change of $R_{DS(on)}$ measured online $\Delta R_{DS(on)}$ and offline $\Delta R'_{DS(on)}$ is shown in Fig. 3.

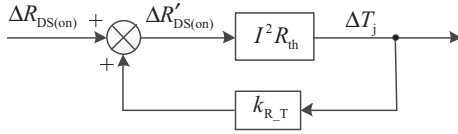


Fig. 3. The relationship between $\Delta R_{DS(on)}$ and $\Delta R'_{DS(on)}$.

In Fig. 3, I is the root mean square (RMS) of the current through the measured MOSFET, R_{th} is the thermal resistance between the MOSFET inner core and heat sink, and k_{R-T} is the temperature coefficient of $R_{DS(on)}$. It can be seen that, with aging, a positive feedback in the shift of $R_{DS(on)}$ is introduced. However, equation (1) is often satisfied:

$$I^2 R_{th} k_{R-T} < 1 \quad (1)$$

So, the system is still stable and $\Delta R'_{DS(on)}$ can be derived as

$$\Delta R'_{DS(on)} = \frac{\Delta R_{DS(on)}}{(1 - I^2 R_{th} k_{R-T})} \quad (2)$$

Therefore, the online measured shift of $R_{DS(on)}$ is higher than its actual shift caused by aging, which means the failure threshold should be increased. In addition, the R_{th} in equation (2) also increases with aging, which leads to $\Delta R'_{DS(on)}$ higher. Of course, the causes of junction temperature rise are much more than these. But to strengthen the confidence level of the research, these factors need to be accounted for.

2) Threshold voltage-based research

The threshold voltage (V_{th}) is one of the basic parameter of MOSFETs. This important parameter is used in two main ways. The first one is for junction temperature measurement of devices, which is usually for thermal management of power modules. The second use concerns the monitoring of the aging of components for reliability reasons. However, if V_{th} is used for real-time health monitoring for components or converters directly, the temperature factor and aging factors should be both considered. It has been mentioned in previous section that V_{th} increases with aging. Furthermore, the increased V_{th} causes more driving loss, which means the junction temperature will rise. In this regard, because V_{th} has a negative temperature

coefficient, the increased temperature will make V_{th} decrease, which may counteract the shift caused by aging. Therefore, when conducting real-time monitoring research, these issues still need to be overcome.

3) Thermal resistance-based research

Solder fatigue causes variation of thermal resistance value R_{th} of device. A thermal resistance-based technique is suitable for monitoring solder fatigue inside the packaging of a power device potentially. However, the challenge is to obtain the internal junction temperature. Three main methods are currently used to evaluate the temperature of power semiconductor devices[14]: optical methods; physical contact methods; electrical methods. The first two methods necessitate visual or mechanical access to the measured chip, which may influence the normal work of the chip. This is the reason why today device temperature evaluation is often carried out using the third method. In this case, the thermal dependence of electrical properties of semiconductor devices is used to determine the temperature. In the literature, the drain-body diode forward voltage, on-state resistance, threshold voltage and saturation current are common used thermo-sensitive electrical parameters (TSEPs) of power MOSFETs [14]. Accuracy and damage robustness are two significant evaluation indexes of the different TSEPs. However, as mentioned in previous sections, these TSEPs all change with the operation time for different degradation mechanisms. At the moment, few papers focus on investigating this issue.

C. The unification and choice of the failure precursors

As mentioned above, different degradation may cause different degradation features. At this point, monitoring a single precursor parameter can only indicate one degradation mechanism, which can't provide a comprehensive health assessment for devices. Thus, it's necessary to find a unified precursor parameter for health monitoring of MOSFETs.

It can be found from the failure precursor parameters listed above:

- 1) An increase in the threshold voltage directly results in an increase in switching time causing additional switching loss.
- 2) The increased gate to drain capacitance means more driving loss.
- 3) The increased on-state resistance means more conduction loss.

Usually, the total loss of a power MOSFET $p_{loss}(t)$ can be expressed as

$$p_{loss}(t) = p_{switching}(t) + p_{conduction}(t) + p_{driving}(t) \quad (3)$$

Where $p_{switching}(t)$, $p_{conduction}(t)$ and $p_{driving}(t)$ are the transient values of switching loss, conduction loss and driving loss, respectively. It can be seen that $p_{loss}(t)$ increases with aging. Meanwhile, a single-chip power module can be drawn in the form of Foster network [15], [16], and a third-order model is shown in Fig.4. R_i and C_i are the thermal resistance and capacitance of the cell i in the Foster network, respectively. T_j

is the junction temperature of the MOSFET and T_{hs} is the temperature of the heat sink.

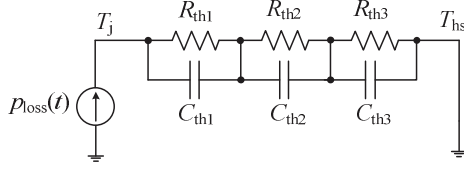


Fig. 4. Typical thermal RC model based on Foster network.

For the MOSFET chip in a steady-state circuit, T_j can be derived as

$$T_j = P_{loss} (R_{th1} + R_{th2} + R_{th3}) + T_{hs} \quad (4)$$

Where P_{loss} is the steady-state value of $p_{loss}(t)$. As analyzed above, P_{loss} and R_{th} both increases with aging. Therefore, T_j will rise certainly. In this regard, the junction temperature can be used as a unified parameter for evaluating the health condition of MOSFETs.

By comparison, the threshold voltage has a good linear relationship with the device temperature ($-2 \sim -6$ mV/ $^{\circ}\text{C}$) at small drain currents ($\square 10$ mA), as well as a high signal-to-noise ratio, and is thus chosen as the failure precursor parameter in this work.

III. CONDITION MONITORING BASED ON THRESHOLD VOLTAGE

A. The principle of condition monitoring based threshold voltage

As concluded above, threshold voltage shifts with aging in MOSFETs, and to eliminate its effect on the result of monitoring, two steps as follows have been taken in this paper.

- 1) Before each startup, V_{th} is measured as the initial value, which is also used for evaluating the degradation of the gate oxide.
- 2) After each shutdown, V_{th} is measured again, and in combination with the initial value, junction temperature can be estimated for the assessment of overall health status.

B. The measurement method threshold voltage

Generally, the threshold voltage measurement is made with a very low current regulation acting on the gate voltage [see Fig. 5(a)] or simply with a connection of the gate and the drain electrodes [see Fig. 5(b)] [14]. The current value is a few mA so as to work as close as possible to the actual threshold voltage. Owing to the complexity of circuit #1 (a current regulation circuit needed) and the particularity of circuit #2 (the grid and the drain electrodes shorted), when it comes to the actual power electronic converters, they are powerless. In this regard, this paper utilizes the unique feature of a Buck converter and proposes a simple method for threshold voltage measurement.

Fig. 6 shows the main circuit diagram of a Buck converter,

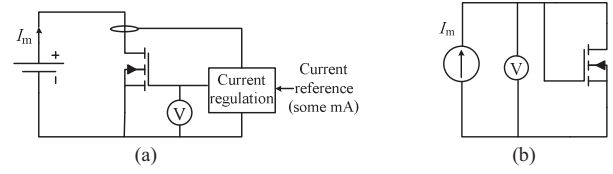


Fig. 5. Common threshold voltage measurement circuits. (a) Measuring circuit #1. (b) Measuring circuit #2.

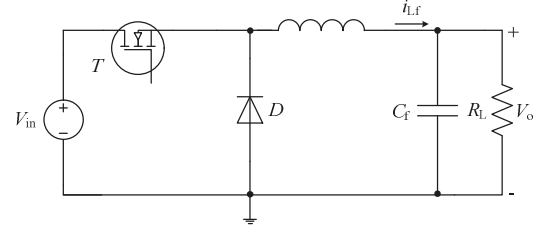


Fig. 6. The main circuit diagram of a Buck converter.

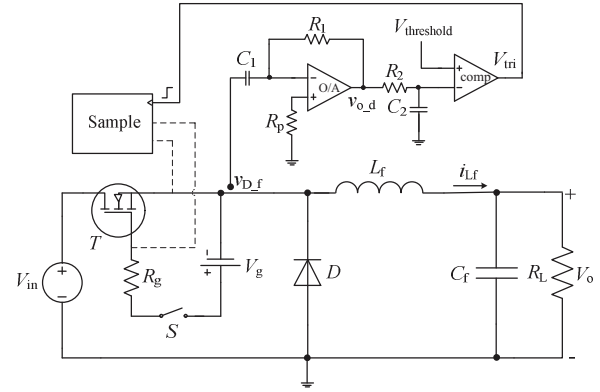


Fig. 7. Proposed circuitry for threshold voltage measurement.

and Fig. 7 illustrates the proposed circuit setup for the threshold voltage measurement of Buck converters. A switch (S) is used as the circuit contactor to disconnect the power the original driving circuit from the converter during measurements. Moreover, a differential circuit (composed by a capacitance C_1 , an op-amp, and two resistances (R_1 and R_p)) is added to detect small current through MOSFET T . Furthermore, a RC buffer circuit (R_2 and C_2) and a comparator circuit are introduced to trigger one sample of the gate to source voltage.

When V_{th} is measured, S is turned on and the voltage source V_g starts charging the gate to source capacitance. Until the voltage between 'g' and 's' v_{gs} reaches the threshold voltage V_{th} , during the time when T operates in saturation mode, T can be equivalent to a current source controlled by v_{gs} and the diode D can be equivalent to its junction capacitor C_D , which is shown in Fig. 8.

The filter inductor L_f is often large, so its flowing current i_{Lf} rises very slowly. For this reason, i_{Lf} can be supposed to be zero. Here, the current through C_D is given by

$$i_D = i_T \quad (5)$$

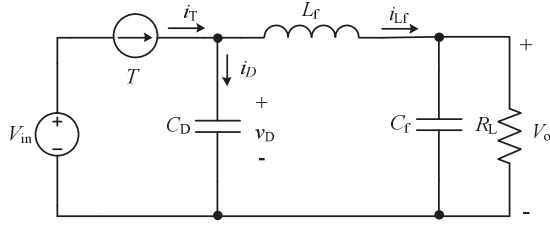


Fig. 8. The equivalent circuit.

where i_T is the current through T . If the initial value of the voltage across diode D ($v_D(t)$) is zero, $v_D(t)$ can be expressed as

$$v_D(t) = \frac{i_T}{C_D} t \quad (6)$$

Furthermore, the output of the differential circuit can be derived as

$$\begin{aligned} v_{o_d}(t) &= -R_1 C_1 H_v \frac{dv_D(t)}{dt} \\ &= -\frac{R_1 C_1 H_v}{C_D} i_T \end{aligned} \quad (7)$$

where H_v is the voltage coefficient. In general, C_D is less than 1nF, so the value of $R_1 C_1 H_v / C_D$ is very large, which means very small current can be detected. When the value of $v_{o_d}(t)$ after the buffer circuit $v_{o_dl}(t)$ reaches the set threshold $V_{\text{threshold}}$, one sampling of v_{gs} will be triggered and the acquired voltage is the measured threshold voltage.

It's important to note that the chosen value of R_1 determines the accuracy of the measurement, while the larger the value of R_1 , the slower v_{gs} rises and the more accurate the measurement is. Furthermore, the chosen value of $V_{\text{threshold}}$ is not only associated with the measurement accuracy, but also concerns the robustness of the measurement.

IV. SIMULATION AND EXPERIMENTAL TEST

The parameters used in this test are listed in Table I. The tested MOSFET is IXFK64N50P, and according to its datasheet, its model has been built by the Power MOSFET Tool in Saber. The threshold voltage of the created model is 4.35V at 25°C and 3.50V at 125°C.

TABLE I. MAIN PARAMETERS OF CIRCUIT

Parameters	Value	Parameters	Value
V_{in}/V	10	$C_f/\mu F$	470
V_g/V	8	$L_f/\mu H$	50
$R_g/k\Omega$	250	$C_1/\mu F$	1
$R_1/k\Omega$	10	$C_2/\mu F$	1
R_2/Ω	500	H_v	1
$R_p/k\Omega$	10	R_L/Ω	100

With the junction temperature of model set to 25°C, S is turned on at 20-millisecond, and the simulation results are shown in Fig. 9. As can be seen from Fig. 9(a), while $V_{\text{threshold}}$ is 0.001V, the measured threshold voltage is 4.335V, which is 0.005V higher than the standard value. Moreover, in Fig. 9(b), the measured value is 4.363V, with a 0.013V higher when $V_{\text{threshold}}$ is set to 0.1V. Therefore, the lower the $V_{\text{threshold}}$, the more accuracy the measured result is.

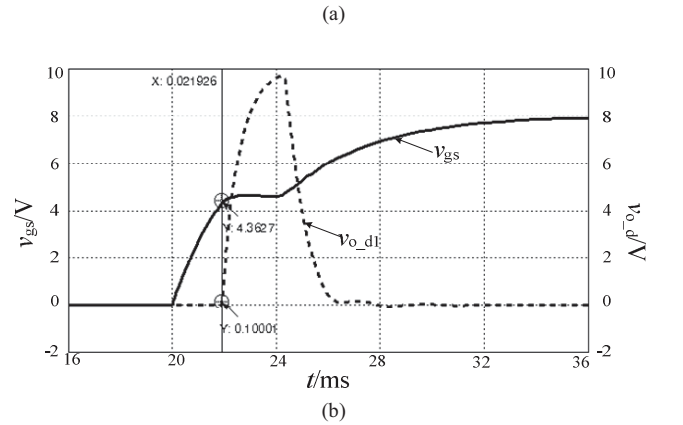
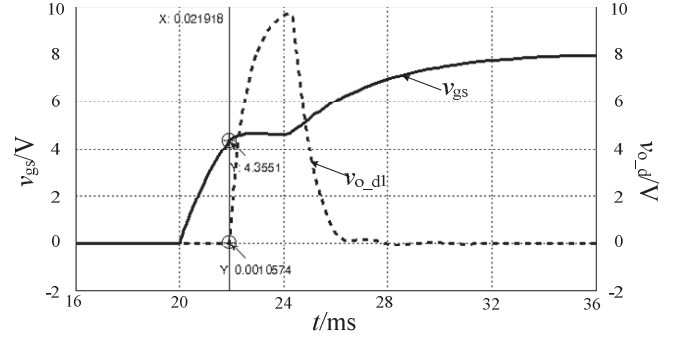
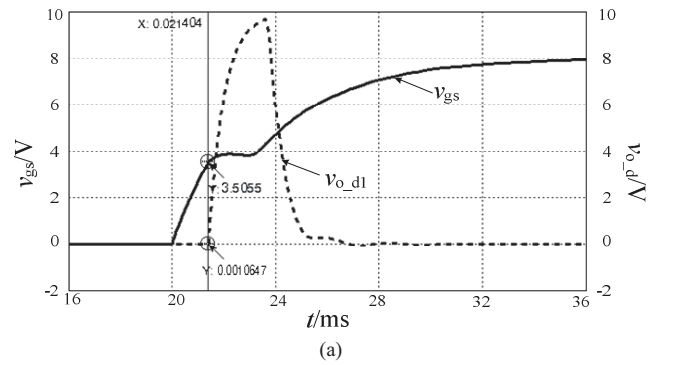


Fig. 9. Simulation waveforms at 25°C. (a) $V_{\text{threshold}} = 0.001V$. (b) $V_{\text{threshold}} = 0.1V$.

Similarly, with temperature set to 125°C, the simulation waveforms are shown in Fig. 10. It can be seen that the measured value in Fig. 10(a) is 3.5055V with a 0.0055V higher and in Fig. 10(b) is 3.514V with a 0.014V higher.



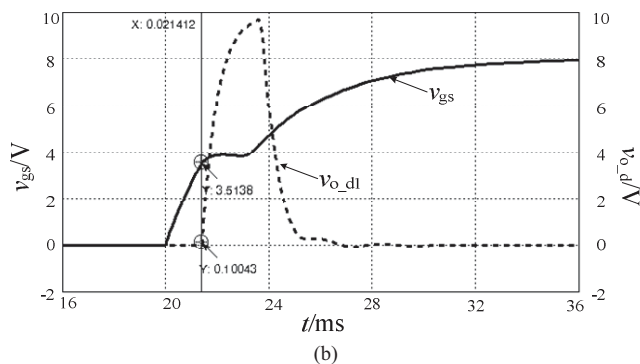


Fig. 10. Simulation waveforms at 125°C. (a) $V_{\text{threshold}} = 0.001\text{V}$. (b) $V_{\text{threshold}} = 0.1\text{V}$.

By comparing the measured results at different temperature, it can be found that the errors are determined by the magnitude of $V_{\text{threshold}}$, nearly irrespective of the junction temperature, which makes the results easy to correct. In this regard, $V_{\text{threshold}}$ can be set to a higher value to improve the robustness of measurement.

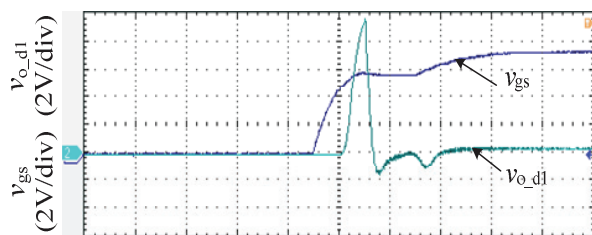


Fig. 11. Experimental waveforms at room temperature (about 25°C)

The experimental waveforms at room temperature (about 25°C) are given in Fig. 11. It can be seen that the experimental waveforms are consistent with the simulation waveforms and the measured V_{th} is 4.40V. In addition, the threshold voltage measured through the method proposed in [17] is 4.41V, close to 4.40V, which verifies the effectiveness of the proposed method.

V. CONCLUSION

The paper has presented a new condition monitoring approach for device reliability in power electronic converters. The novelty lies in the unification of failure precursors and the way of threshold voltage measurement for MOSFETs in a Buck converter.

In this paper, the origin of power MOSFETs failure and the measurable failure precursors which can quantify the level of aging have been described and one common degradation feature was found: causing the junction temperature to rise. Thus, the junction temperature was chosen as an overall indicator for health monitoring and the threshold voltage was proven to be an important temperature sensitive electrical parameter to detect the degradation of the power MOSFETs. Given this, a monitoring method based on the threshold voltage has been proposed, which can eliminate the effect of device aging on junction temperature estimation. Besides, a new

threshold measurement method was proposed for Buck converters. The validity of the proposed measurement method has been confirmed by simulation and experiments.

The proposed technologies are based on Buck converters. However, the health monitoring scheme also applies to other converters and the threshold measurement method can also be promoted to other buck-derived converters. In the future work, the whole condition monitoring scheme will be accomplished.

REFERENCES

- [1] E. Wolfgang, "Examples for failures in power electronics systems," presented at the ECPE Tutorial 'Rel. Power Electron. Syst.', Nuremberg, Germany, Apr. 2007.
- [2] M. Held, P. Jacob, G. Nicoletti, P. Scacco, and M. H. Poehch, "Fast powercycling test of IGBT modules in traction application," in Proc. Int. Conf. Power Electron. Drive Syst., 1997, pp. 425–430.
- [3] W. Wu, L. Wu, H. Zhang, L. Dong, P. Jacob, and M. Held, "A study of EOS failures in power IGBT modules," in Proc. 5th Int. Conf. Solid-State Integr. Circuit Technol., 1998, pp. 152–155.
- [4] G. Coquery and R. Lallemand, "Failure criteria for long term accelerated power cycling test linked to electrical turn off SOA on IGBT module. A 4000 hours test on A-3300 V module with AlSiC base plate," Microelectron. Rel., vol. 40, no. 8–10, pp. 1200–1270, 2000.
- [5] M. Mermet-Guyennet, X. Perpiñá, and M. Piton, "Revisiting power cycling test for better life-time prediction in traction," Microelectron. Rel., vol. 47, no. 9–11, pp. 1690–1695, 2007.
- [6] H. Berg and E. Wolfgang, "Advanced IGBT modules for railway traction applications: Reliability testing," Microelectron. Rel., vol. 38, no. 6, pp. 1319–1323, 1998.
- [7] N. Patil, D. Das, K. Goebel, and M. Pecht, "Failure precursors for insulated gate bipolar transistors (IGBTs)," in Proc. ISPS Conf. Rec., Prague, Czechoslovakia, Aug. 2008, pp. 107–112.
- [8] S. Yang, D. Xiang, A. Bryant, P. Mawby, L. Ran, and P. Tavner, "Condition monitoring for device reliability in power electronic converters: A review," IEEE Trans. Power Electron., vol. 25, no. 11, pp. 2734–2752, Nov. 2010.
- [9] D. A. Grant and J. Gowar, Power MOSFET-Theory and Applications. New York: Wiley, 1989.
- [10] S. Saha, J. R. Celaya, V. Vashchenko, S. Mahiuddin, and K. F. Goebel, "Accelerated aging with electrical overstress and prognostics for power MOSFETs" in Energytech, 2011 IEEE, vol. 10, no. 1109, pp. 1–6.
- [11] Kyung Ki Kim, Wei Wang, and Ken Choi, "On-chip aging sensor circuits for reliable nanometer MOSFET digital circuits," IEEE Trans. Circuits and Systems., vol. 57, no. 10, pp. 798–802, Oct. 2010.
- [12] S. S. Mahiuddin, "Modeling of the impact of electrical stressors on the degradation process of Power MOSFETs," M.S. thesis, Dept. Elec. Eng. San Jose State Univ., San Jose, CA, USA, 2011, Paper 3943.
- [13] T. Azoui, P. Tounsi, Ph. Dupuy, J. M. Dorkel, and D. Martineau, "Numerical and experimental results correlation during power MOSFET ageing," in Proc. 13th Int. Conf. Therm., Mech. Multi-Phys. Simul. Experiments Microelectron. Microsyst., 2012, pp. 1/4–4/4.
- [14] D.-L. Blackburn, "Temperature measurements of semiconductor devices—A review," in Proc. 20th Annu. Semicond. Therm. Meas. Manage. Symp., San Jose, CA, Mar. 11–24, 2004, pp. 70–80.
- [15] Y. Yu, T. Lee, and V. A. Chiriac, "Compact thermal resistor-capacitor network approach to predicting transient junction temperatures of a power amplifier module," IEEE Trans. Compon. Packag. Technol., vol. 2, no. 7, pp. 1172–1181, Jul. 2012.
- [16] K. Gorecki and J. Zarebski, "Nonlinear compact thermal model of power semiconductor devices," IEEE Trans. Compon. Packag. Technol., vol. 33, no. 3, pp. 643–647, Sep. 2010.
- [17] H. Chen, B. Ji, V. Pickert, and W. Cao, "Real-time temperature estimation for power MOSFETs considering thermal aging effects," IEEE Trans. Device Mater. Rel., vol. 14, no. 1, pp. 220–228, Mar. 2014.